CHALMERS

Calculation of Welding Deformations in a Pipe Flange

Master's thesis in Applied Mechanics

MAGNUS RHODIN

Department of Applied Mechanics
Division of Material and Computational Mechanics
CHALMERS UNIVERSITY OF TECHNOLOGY
Gothenburg, Sweden 2012
Master's thesis 2012:31

MASTER'S THESIS IN APPLIED MECHANICS

Calculation of Welding Deformations in a Pipe Flange

MAGNUS RHODIN

Department of Applied Mechanics
Division of Material and Computational Mechanics
CHALMERS UNIVERSITY OF TECHNOLOGY

Gothenburg, Sweden 2012

Calculation of Welding Deformations in a Pipe Flange

MAGNUS RHODIN

Master's thesis 2012:31
ISSN 1652-8557
Department of Applied Mechanics
Division of Material and Computational Mechanics
Chalmers University of Technology
SE-412 96 Gothenburg
Sweden
Telephone: +46 (0)31-772 1000

Chalmers Reproservice
Gothenburg, Sweden 2012

Calculation of Welding Deformations in a Pipe Flange

Master's thesis in Applied Mechanics
MAGNUS RHODIN
Department of Applied Mechanics
Division of Material and Computational Mechanics
Chalmers University of Technology

Abstract

Reducing post welding processing of flanges due to distortion is a big cost and time saver for the oil and gas industry. Vector Technology Group AS experience different deformations in flange welded to pipes designs, and the reason for these deformations are crucial when designing to reduce them. Two flange designs are provided and the investigation is made with the commercial software ANSYS, where the entire welding procedure is modeled. The flanges are welded on to a pipe of the same diameter and thickness using TIG welding, experimental results are only available as measurements of displacements and rotations at certain locations for the flange.
Since ANSYS is not an established welding simulation software, a benchmarking is made to a well-known FE-simulation from 1978. The software ANSYS works with some restrictions when modeling welding, for example the element birth and death techniques incorporated makes the handling of adding filler material easy, but when modeling solid-solid phase changes the software does not seem to cope.
In the present simulations, the flanges are modeled in two-dimensional axisymmetric models with different boundary conditions in order to simulate different techniques of fixing the work pieces while welding. An elastic analytical estimation, measurements provided and ANSYS results show that the CRYO model will be the design to withstand deformations the best. However the results also show that it is equally important how the flange and pipe are fixed in place when welding, and specific procedures for the welding should be developed when working with the desired high precision in positioning the flange.

Keywords: Finite element method, welding, residual deformations, ANSYS.

Preface

This thesis is made as the concluding part of a five year program at Chalmers University of Technology in Mechanical engineering and leads to the degree of Master in Science. The work was carried out at the office of EDRMedeso in Gothenburg in collaboration with Vector Technology Group AS in Norway, during the spring of 2012.

Thanks to EDRMedeso and Vector for giving me the opportunity to conduct this project and utilize all the resources at hand. Special thanks to Chouping Luo and Frode Halvorsen at EDRMedeso for crucial support and guidance in ANSYS throughout the entire project. I am also extremely grateful for the support and help from my examiner Professor Lennart Josefson at Chalmers. The guidance by Lennart concerning welding simulations have been vital for the whole thesis.

But most of all, I am extremely grateful to my friends and family, and especially Sofie, for the support and patience during my five years at Chalmers. You helped me more than you realize.

Magnus Rhodin

Nomenclature

c	$=$	thermal capacitivity (J/kg°C)
λ	$=$	thermal conductivity (W/m°C)
ϵ	$=$	thermal dilatation strain (-)
u	$=$	heat content (J)
η	$=$	arc efficiency (-)
U	$=$	voltage (V)
I	$=$	current (A)
v	$=$	welding speed (m/s)
t	$=$	time coordinate (s)
ρ	$=$	density (kg/m^3)
L	$=$	latent heat (kJ/kg)
α	$=$	thermal expansion coefficient (1/°C)
E	$=$	elasticity modulus (GPa)
ν	$=$	Poission's ratio (-)
H'	$=$	plastic hardening modulus (GPa)
E_t	$=$	tangent hardening modulus (GPa)
T	$=$	temperature (°C)
θ	$=$	cross sectional rotation (°)
H	$=$	cross sectional stiffness (m^4)
M	$=$	evenly distributed moment per unit length(Nm/m)
r	$=$	radius (m)

Contents

1 Introduction

1.1 Background

The oil and gas industry is an important and a key player in the world today. The industry is highly complex, involves substantial amount of capital, which then sets high demands for the services and materials used in the production processes. Welding in this industry is a key element in joining components in all areas.

Pipe flanges are often used to connect pipes to each other or to other equipment. Since different substances travel through the pipes flanges at high speed and pressure the demands on these components are high, hence narrow tolerances on the flanges and pipes must be used. When welded on to the pipes the flanges becomes deformed and no longer meet the requirements and they often have to be processed once more after welding to ensure the quality and fit of the connection. This extra processing of the connection costs both time and money when installing a new pipeline and it is therefore preferable to avoid it.

Two existing types of flanges have been provided along with material data, welding specifications and documentations of where the unwanted deformations occur. The two different flange geometries behave differently after welding, and the reason for this is of great interest for future design and manufacturing.

1.2 Objectives

There are two main objectives with this Thesis:

- To asses the welding simulation capabilities of the commercial software package ANSYS.
- To evaluate two different pipe flange designs, undergoing welding, with respect to residual welding deformations.

This means developing two FEM models within ANSYS simulating the entire welding process.

2 Theory

This chapter is intended to present the theory around the process of welding and how to simulate it using the finite element method. The complex nature of welding is explained first and then the different ways of handling these complexities in a computational finite element model is explained.

2.1 Welding

Welding is a complex and coupled procedure. There is rapid heating of material which causes it to melt and often base and filler material gets mixed together. This will affect the material properties once the material has hardened, partly because of the mix and also because of the thermal cycle the material have experienced. The couplings in a welding process presented by [1] can be seen in Figure 2.1.1, together with the explanation of each coupling in Table 2.1.1.

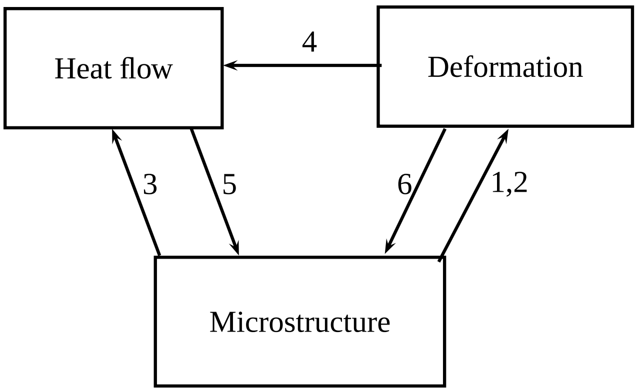

Figure 2.1.1: *Phenomena occuring during welding [1].*

Table 2.1.1: Coupling explanations to figure 2.1.1 [1].

Coupling #	Explanation
1a	Thermal expansion depends on microstructure of material.
1b	Volume changes due to phase changes.
2a	Plastic material behavior depends on microstructure of material.
2b	Elastic material behavior depends on microstructure of material.
3a	Heat conductivity and heat capacity depend on microstructure of material.
3b	Latent heats due to phase changes.
4a	Deformation changes thermal boundary conditions.
4b	Heat due to plastic dissipation (plastic strain rate).
4c	Heat due to thermal strain rate.
4d	Heat due to elastic strain rate.
5	Microstructure evolution depends on temperature.
6	Microstructure evolution depends on deformation.

This thesis concerns fusion welding with the addition of filler material, were the filler material and the base material melts together. The process is complex, since it involves high temperatures and high temperature gradients, an uncertain mixture of metals and leaves residual stresses in the material which is hard to determine a priori. In [2] different welding techniques and their characteristics are described together with other useful information regarding welding i.e. different joint types.

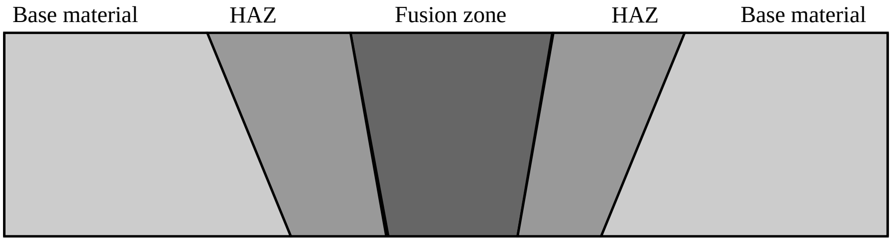

Figure 2.1.2: *Zones close to the weld.*

Important areas of the weld are shown in Figure 2.1.2. The fusion zone is the area where the filler material and a small part of the base material melts and gets mixed together, and will act as fluid for a short period of time. This will change the microstructure of the material, since two materials are mixed and undergo heating and cooling. To reduce the microstructure change in the fusion zone due to two materials mixing together it is usually advisable to use a filler material with similar compositions as the base material. The Heat-affected Zone(HAZ), is the part next to the fusion zone, light grey area in the figure. This area is not melted nor mixed with the filler material, but still affected by the heat so that the microstructure and material properties is changed. The size and shape of both the fusion zone and the HAZ is dependent on a number of parameters, among those are the welding process(TIG,MIG,SAW etc.), welding parameters(current, voltage, welding speed), material properties etc. The base material, the lightest grey in the figure, is unaffected when considering the microstructure. It is of course affected by heating, but not to that extent that the material properties change during the welding process. The HAZ and base material act as cooling sources together with the surroundings to cool the workpiece.

Residual stresses and deformations occur in a welded structure because of the local rapid heating and cooling of the material and the resulting plastic deformation. When a small part of the material is heated it will try to expand according to Equation 2.1.1, where the volumetric thermal expansion coefficient is assumed not to be temperature dependent.

$$
\begin{aligned}
\Delta V &= \alpha_v \cdot \Delta T \cdot V \qquad (2.1.1)\\
where&\\
\Delta V &= Volume\ change\\
V &= Original\ volume\\
\alpha_v &= Volumetric\ thermal\ expansion\ coefficient\\
\Delta T &= Temperature\ change
\end{aligned}
$$

The surrounding material not heated, or not heated with the same intensity, will prevent this expansions to some extend and compressive stresses will be formed inside the heated part of the material. These deformations and stresses will disappear from the material if it is only compressed elastically, so when cooled down to the starting temperature the initial state of the material is in place again. However, if the rapid heating and expansion would cause plastic deformations of the heated material, i.e. the stresses would exceed the yield limit, and plastic strains would be introduced inside the material. When cooled the material is going to contract, and eventually it will contract to a smaller volume than before the heating or at least try to, the surrounding materials prevents this. So when the material once again arrives at the initial temperature, tensile stresses will remain in the heated part and compressive stresses in the surroundings. Other phenomena occurring during the heating and cooling such as phase transformation can also affect the expansion/contraction of the material and further induce irreversible deformations affecting the residual stresses. The effect of the phase transformations on the residual stresses depend on a number of things, i.e. material, peak temperature etc. These residual stresses will then account for the deformations occurring after welding and depending on the structure and material properties these will be different.

2.2 Finite Element Simulation of welding

The ability to simulate welding processes has its origin in the 1930s with analytical theories, which was refined during the following two decades. Due to limited computer advancement there where only two-dimensional FE-analysis conducted until the mid 1980s. Since then more and more complex numerical models have been used to analyze the welding process, where the finite element method is especially represented.

Since the welding process is a complex and coupled one, as discussed previously, simulating the process with the Finite element method can be very complex as well. Therefore to make it worthwhile, both in terms of calculation time and pre-processing time, to analyze a weld, certain simplifications and approximations are usually made. Figure 2.1.1 and Table 2.1.1 is the starting point from which simplifications and approximations are made. The first simplification usually made is to simplify the microstructure dependencies of all couplings that have them(1a, 2a,2b & 3a) and assume that the material properties only depend on temperature [3]. It is a very common approach and can be considered well-established [3]. The first coupling, both a and b, is essential to solve the mechanical field. Volume changes due to phase changes are sometimes ignored due to small phase changes or none, they are however especially important when modeling ferritic steels [3]. Latent heats due to phase changes, coupling 3b, are often included and can be of great importance when modeling certain materials, especially ferritic steels. The latent heats of both solid-solid phase change and solid-liquid phase change are common to include in the heat capacities, there are finite element packages that allows you to specify the latent heat of fusion and the program handles it by itself. If not, the latent heats give effective heat capacities according to Equation 2.2.1 [4].

$$\begin{aligned}
c_{eff} &= c_s(T < T_s) \\
c_{eff} &= c_f + \frac{L}{T_l - T_s}(T_s < T < T_l) \\
c_{eff} &= c_l(T_l < T) \\
where & \\
c &= Specific\ heat \\
T_s &= Solidus\ temperature \\
T_l &= Liquidus\ temperature \\
L &= Latent\ heat
\end{aligned} \tag{2.2.1}$$

When including the latent heats in the heat capacities the solid-solid latent heats pose minimal problems, but the solid-liquid latent heats are so much larger in comparison to the heat capacity so that nonlinearities appear and it can often cause convergence issues, especially if the temperature interval between the solidus and liquidus temperatures is small. One way to overcome this would be to increase the temperature range at which this heat is absorbed/released, or it is possible to use a different approach called the enthalpy method, which is used by [5, 6]. With this method the enthalpy or heat content is used as the primary variable to solve for, according to Equation 2.2.2.

$$H(T) = \int_0^T \rho c dT \tag{2.2.2}$$

By applying this method the nonlinearities due to the latent heats will be greatly reduced during the phase transformations which provides a more stable simulation. Not all finite element packages can apply this method but some of them can, ANSYS is one of them. The contributions from couplings 4a-4b are considered small enough to be ignored. This means that the modeling becomes an uncoupled and quasistatic one. Where the thermal analysis is completed and the mechanical one is conducted afterwards with the temperature history from the thermal analysis as the only load. When coupling 4a is important the most common and convenient way of including it is by using the so called staggered approach. Since the microstructure of the material is ignored, coupling 5 essentially reveals that the mechanical properties depend on temperature. The deformations influence on the stresses, coupling 6, is in the order of 10^{-3} and has not yet been implemented in welding simulations [1].

When both the base and filler material melts as the arc passes, the two mix together and are at this stage fluids which is going to cause a convective stirr. Modeling this accurately would require a fluid flow model, that means further complicating the computational model. So to keep the complexity at a reasonable level many use a artificially high thermal conductivity above the melting temperature [5, 7, 8], to account for this effect.

The amount of energy supplied and the way it is supplied is important. This will have a great influence on the molten zone and HAZ. An analysis where results near the weld are of importance the procedure of applying the correct amount in the right way becomes more important. Therefore some kind of verification of the supplied energy is needed. If experimental data is present then a comparison and tuning of the model according to this is essentially the best. Either by mounted thermocouples to compare measured and calculated temperatures. Or if possible, look at the shape and measure the extend of the molten material and HAZ from the experimental weld by cutting a cross section.

Another important part in simulating welding is the handling of adding the extra material/filler material that is not present from the beginning. There are two well established methods of doing this, either the filler material is included from the beginning or the model is extended during the analysis [9]. The first one is named *quiet elements*, where the filler material is included but given material properties so that they do not affect the rest of the model. Finding the material properties suitable, which does not affect the surroundings or gives numerical problems, is an iterative procedure. In [10] it was found that Young's modulus of 2GPa worked for their repeat of [5], [7] sets the temperature in the filler material elements to a high temperature where the material properties are low enough to consider the elements as inactive.

The second approach where the elements are excluded from the model until the filler material is supposed to be added is named *inactive elements*. The model grows with each weld pass and is complete after the last weld pass. This is a more correct approach, but is more problematic to implement. The biggest issue is that elements that are not included from the beginning does not follow the models deformations and when included the elements will most likely become highly distorted. To overcome this would imply a lot of manual work or advanced software. The quiet element method follows the deformed geometry and this problem is avoided in an easier way, to the expense of small stresses and strains in a supposed stress and strain free material. In [9] it was found that the difference between the two approaches are small, however it was also found that the inactive elements approach required shorter computation time.

The first approach is used in this thesis, since it is easier to implement and still gives equally accurate results. Additionally ANSYS also provides tools/commands which are very useful for this approach. It incorporates something called element birth and death, through commands EALIVE and EKILL [11], respectively. This works in a similar way to assigning a material low material properties, when elements are 'killed' using EKILL command, these elements remain in the model but with a low stiffness (or conductivity etc.) by multiplying its stiffness(or conductivity etc.) matrix with a small value called ESTIF. The value of ESTIF is 1.0E-6 by default but can be set by the user in order to tune the model to give accurate results. By applying EKILL to elements all stresses and strains are set to zero, and then activated again using EALIVE command. One important note is that in order for the elements not to be reactivated with larger thermal strains the elements reference temperature needs to be set to the temperature at which they are reactivated.

This thesis only concern two-dimensional simulations of welding, which is a common way of reducing the size of the model and therefore also the computational effort needed to solve it. This can have implications on the results depending on what the analysis is after. By reducing a model to two dimensions and analyzing a cross-section the model fails to account for the heat conduction in the welding direction.

3 The Andersson model

In this chapter the Andersson simulation in [5] is repeated in order to acquire practical knowledge of welding simulations in general and in ANSYS especially. Andersson conducted the welding experiment and simulation in 1978 and achieved good correlation between the results. Anderssons work is also chosen since it contains enough data to be reproduced and it is a well-known work which has been repeated by others e.g. [10, 12].

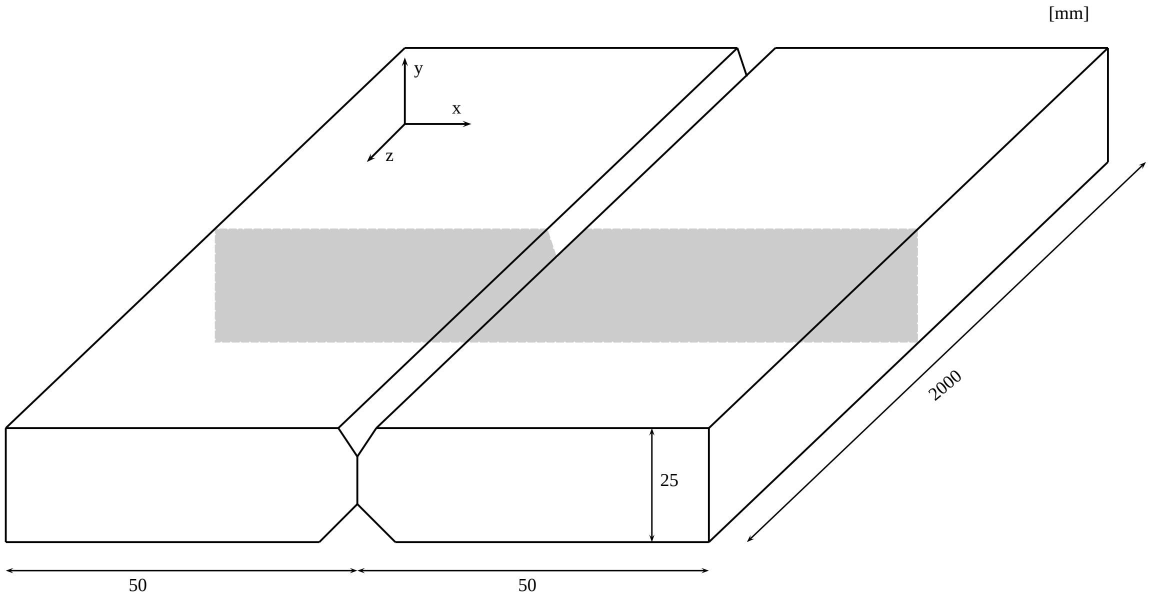

Figure 3.0.1: *Overview of the two plates to be welded together.*

Andersson analysed a stationary cross section of two plates that was being welded together by submerged-arc welding (SAW). The error introduced by simulating two-dimensionally is estimated in the paper and it is found to be negligible except in the area very close to the weld. The two plates are 25x500x2000 mm see Figure 3.0.1, where the shaded area is the cross section to be analyzed. Which is also shown separately in Figure 3.0.2. Note that the plates where only welded together on the top side, even though there is a groove on bottom side as well. The two plates where tack-welded and stress relief before welded together completely using submerged arc welding, with three electrodes. The analysis is made in an uncoupled fashion, since this is an approach that requires less computer resources and it is also the way Andersson originally did it.

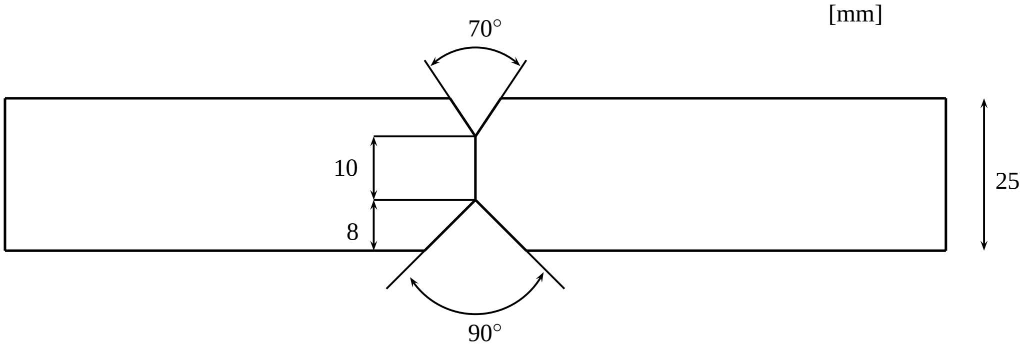

Figure 3.0.2: *Cross section to be analyzed.*

3.1 Material properties

The material properties is gathered from Anderssons [5] diagrams and are presented in Figures 3.1.1-3.1.2. The solidus temperature is assumed to be 1480°C and the liquidus 1530°C, for both weld and base material. To account for the stirror effect in the weld puddle the thermal conductivity is set to a high value, 230 W/m C, at temperatures exceeding the melting temperature. To account for the phase changes in the material the latent heat of fusion $L = 260$ kJ/kg, and is incorporated in the specific heat according to Equation 2.2.1 [4]. This stores the fusion energy when heated and releases it when cooling between T_s and T_l. This is explains why both the thermal conductivity and the specific heat drastically disappears in Figure 3.1.2.

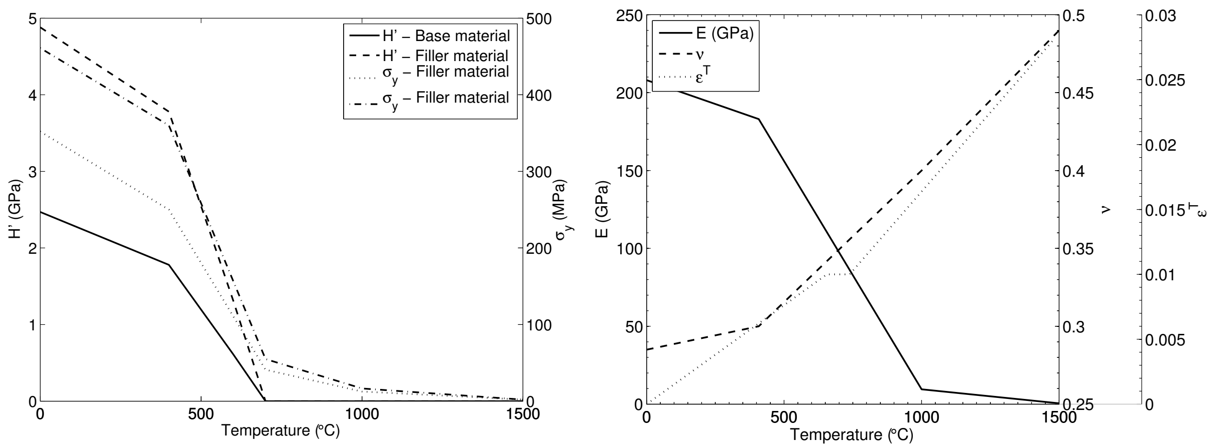

(a) *Yield stress and Hardening modulus.* (b) *Young's modulus, Poisson's ratio and thermal dilatation.*

Figure 3.1.1: *Mechanical properties for the base and filler material used [5].*

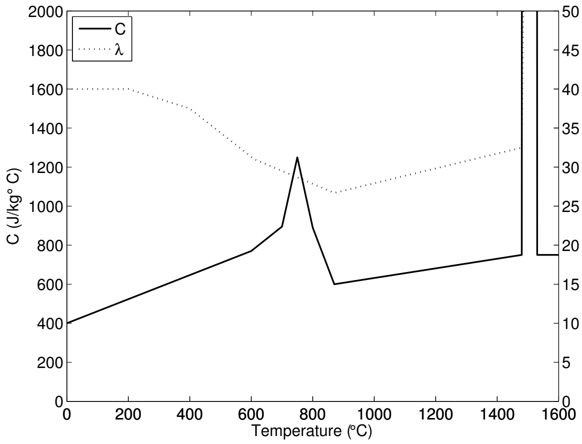

Figure 3.1.2: *Thermal properties for the base and filler material used [5].*

Andersson used thermal dilatation, ϵ^T, as shown in Figure 3.1.1b. This material property is not supported in ANSYS, and is converted to thermal expansion, α, through the relationship in Equation 3.1.1. The same is true for the plastic hardening modulus, H', which is converted to the tangent modulus, E_t, through Equation 3.1.2 which ANSYS uses.

$$\epsilon^T = \int \alpha(T) dT \tag{3.1.1}$$

$$E_t = \frac{H'E}{E + H'} \tag{3.1.2}$$

Andersson included three different thermal dilatation curves depending on the peak temperature of the elements in order to capture the solid-solid phase changes more correctly, this is not implemented in the present analysis. It was deemed to acquire too much time to implement, considering it is not needed for the flange analysis which is the main objective of this thesis. On top of that the one thermal dilatation curved that is shown in Figure 3.1.1b, could not be implemented either. The thermal expansion had to be kept at a constant level of 1.40845e-5, from 0 to 1300° and from there drop to zero at 1400°. This value is the correct one according to the thermal dilatation curve, but only for the first 710°, including the phase change between 710 to 800° creates convergence problems not possible to overcome. This means that no phase change effects are accounted for, and that mechanical effects above 1400° are also ignored.

3.2 Finite element model

Since the cross section is symmetric only one half of it is analyzed in this study. The finite element model used, in both the thermal and mechanical analysis is shown in Figure 3.2.1. It consists of 4581 elements and 4889 nodes. A mesh convergence study showed that increasing the mesh density did not present any change in results. In the thermal analysis ANSYS element PLANE55 is used, which is a 4-node 2-D thermal solid, and for the mechanical analysis the 2-D 4-node PLANE182 is used. Theses element types both use four integration points, however in the mechanical analysis the PLANE182 element needed to use reduced integration with hourglass control in order to prevent volumetric locking. This reduces the number of integration points to one in the mechanical analysis.

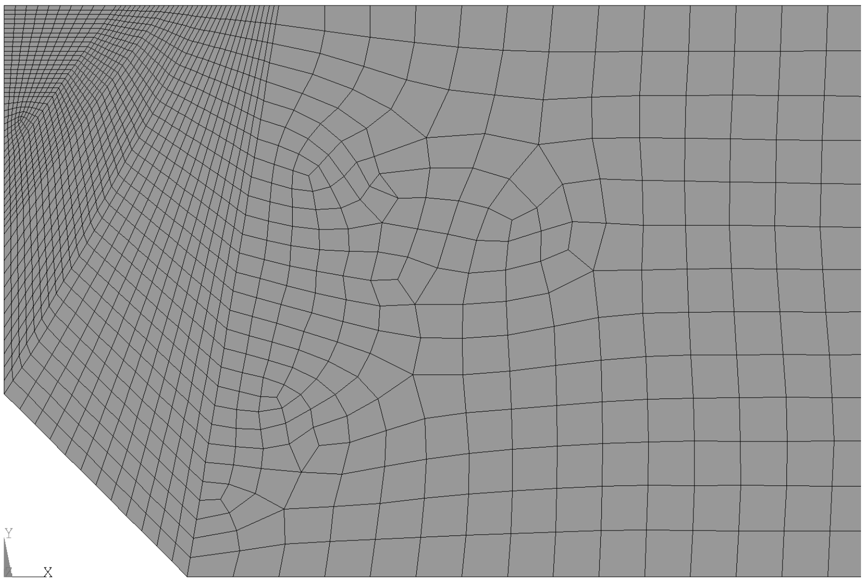

Figure 3.2.1: *Finite element mesh used for part close to the weld.*

3.3 Thermal analysis

The thermal analysis is of great importance when simulating welding, since it is the only load for the latter mechanical analysis. It is also very hard to capture the exact energy input since it is hard to know how much energy that is supplied from the welding rod to the material or the ambient, and in addition to that the current and voltage of the weld equipment can be hard to keep at a constant level.

The thermal energy is supplied to the weld by three electrodes followed closely by each other, which are active for one second each and their respective parameters are found in Table 3.3.1. The arc efficiency is assumed by Andersson to be 0.9 for submerged arc welding.

Table 3.3.1: Welding parameters.

Electrode no.	I ampere	U volt	v m/s	Heat input kJ/mm
1	800	30	0.025	0.960
2	900	38	0.025	1.368
3	900	44	0.025	1.584

The heat input to the model is divided in to two parts, where the first one is the heat content in the filler material which is set to $T_{pre} = 1800°$ when deposited and the second is a constant heat generation element body force through the BFE command in ANSYS [11], with unit W/m^3. The three electrodes passing is simulated in three steps, according to Figure 3.3.1, each active for one second each. At the beginning of the analysis weld pass 1 is active with a heat source while the other two are ”quite” using ANSYS EKILL command. In the second step, weld pass 2 is brought alive using the EALIVE command and its corresponding heat input is applied, and the same procedure is repeated for the third and last weld pass. The matrix multiplier ESTIF used by ANSYS to ”kill” elements is set to 1E-3.

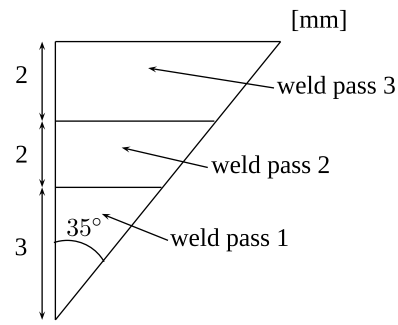

Figure 3.3.1: *Weld area divided in three weld passes.*

The total heat input to the work piece for each weld pass is calculated using Equation 3.3.1 and the values in Table 3.3.1.

$$Q_{tot} = \frac{U \cdot I \cdot \eta \cdot l}{v} \qquad (3.3.1)$$

where

$$\eta = arc\ efficiency$$
$$l = length\ of\ weld\ pool$$

The total heat input is reduced by the amount equal to the heat content in the filler material at T_{pre} according to Equation 3.3.2, and then divided by the filler material volume for the corresponding weld pass to which the heat is applied and the time the electrode is active, as Equation 3.3.3 describes.

$$u_{filler} = T_{pre} \cdot V_{filler} \cdot c_p(T_{pre}) \cdot \rho \tag{3.3.2}$$

$$q = \frac{Q - u_{filler}}{V_{filler}} \tag{3.3.3}$$

Heat is assumed to leave the plate during and after welding from all outside edges due to convection and radiation, where the convective heat transfer coefficient is set to 12 W/m^2 and the emissivity to 0.004939 together with the stefan boltzmann constant of 5.6704E-8. After the three weld passes the plate is cooled to room temperature (20°C).

3.4 Mechanical analysis

For the mechanical analysis generalized plane strain is assumed, and the temperature from the thermal analysis is applied as a the only load. To model that the filler material is introduced in melted form when the weld passes are brought "alive", the filler material uses a reference temperature equal to T_{pre}. The plate is fixed in the bottom right corner of the cross section in order to prevent rigid body motion during the simulation.

3.5 Results

In this section the results are compared to that of Andersson [5], from his paper both the experimental and FEM results is included for the residual stresses. To verify the thermal results Andersson installed three thermocouples in the plate before doing the experiment. The placement of these thermocouples are shown in Figure 3.5.1, and in Figure 3.5.2 the results from the experiment and the FEM results from ANSYS is shown.

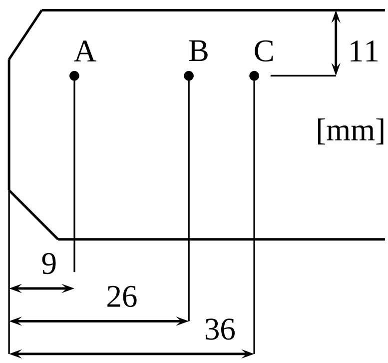

Figure 3.5.1: *Positions of the three thermocouples installed.*

The residual stresses are compared in Figure 3.5.3 and 3.5.4, for the upper and lower side of the plate respectively. Andersson mounted strain gauge rosettes on both the upper and lower surface of the plate to measure the residual stresses after the plate had cooled to room temperature using the Gunnert drilling technique. The area closest to the weld on the upper surface is the most difficult to model, and the model deviates in this area for σ_x. The reason for the general deviation from Anderssons simulation is most likely because of the fact that the thermal dilatation, and therefore also the solid to solid phase changes, could not be included in the model.

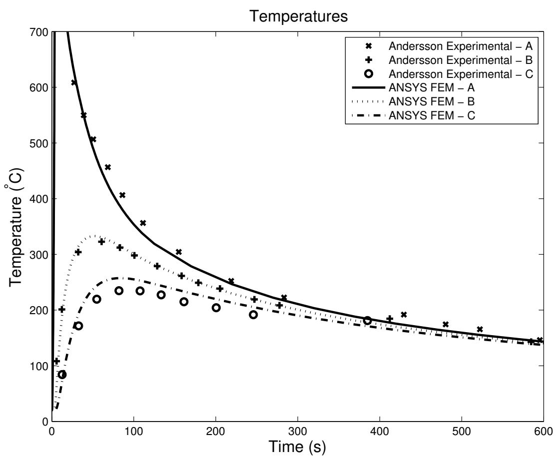

Figure 3.5.2: *Calculated temperatures compared to measured values.*

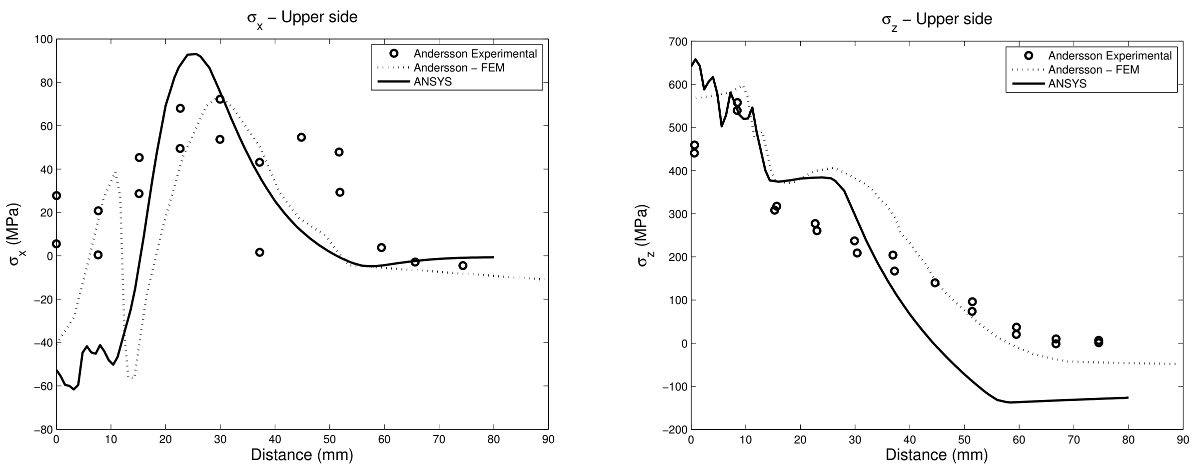

(a) σ_x

(b) σ_z

Figure 3.5.3: *Stress results for the top surface.*

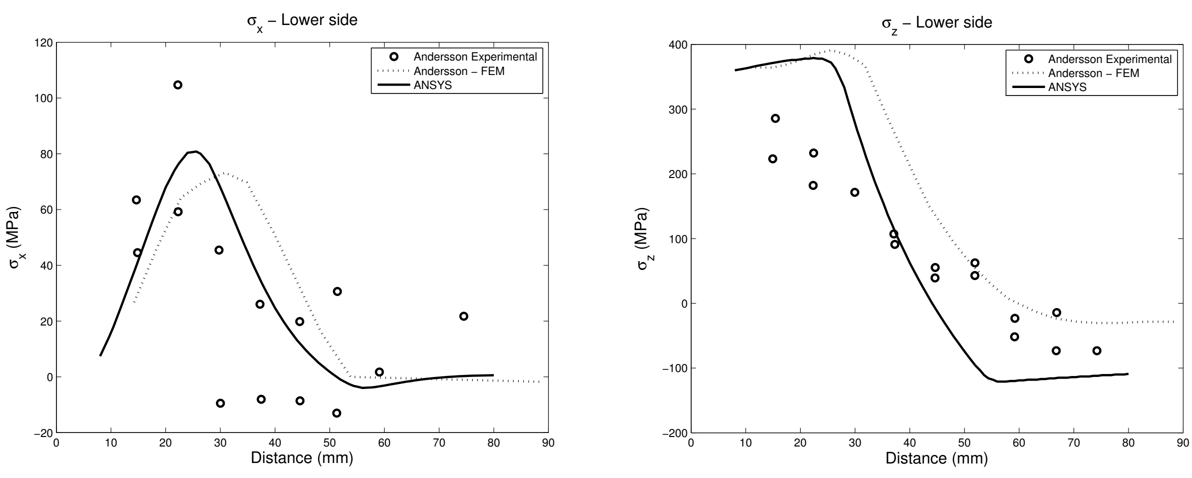

(a) σ_x

(b) σ_z

Figure 3.5.4: *Stress results for the bottom surface.*

4 Pipe flange model

In this chapter the pipe flanges manufactured by VECTOR, will be described and analyzed. Two different model geometries have been provided, their axisymmetric representation in ANSYS can be seen in Figure 4.0.1a and 4.0.1b for CL150 and CRYO CL150 respectively. The difference in the two models is small, CRYO CL150 is slightly taller and has a smaller groove for a gasket. These differences gives rise to different magnitudes of distortion after they have been welded to a pipe. The flange and pipe are specified to be welded together with welding process 141, which is Tungsten Inert Gas welding (TIG) [2].

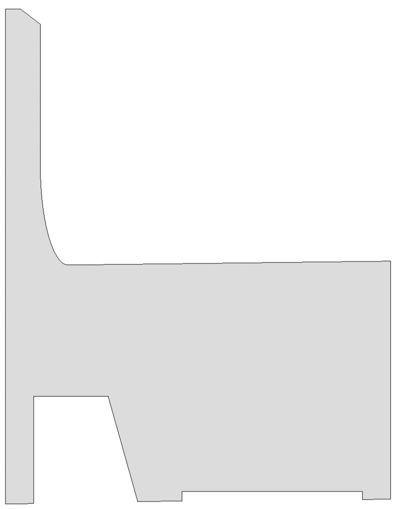

(a) *CL150*

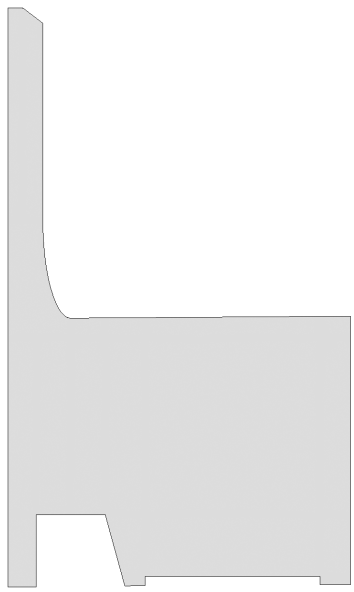

(b) *CRYO CL150*

Figure 4.0.1: *Axisymmetric geometries of flanges.*

The analysis covers both models being welded to a pipe of the same inner(211.6 mm) and outer(219.1 mm) diameter as the flanges, with a length of 4.4 m. The weld groove is the same for both models, as seen in Figure 4.0.2, and there are three weld passes present[13]. The analysis of both flange are made for different boundary conditions used to hold the pipe and flange in place while welding, to investigate the impact this has on the distortions. There are three possibilities:

1. The pipe and flange are tack welded which means that a minimum amount of support is needed to keep the parts in place.

2. The flange is bolted, using the holes around its circumference, to an adjustable work bench and the pipe is brought in at the same height.

3. A Chuck is placed inside, to apply a pressure and support not directly on the weld but in its vicinity around the circumference for both the pipe and flange.

The thesis will cover option one and two, option three is outside the scope of this thesis since it will make an already complex simulation even more complex.

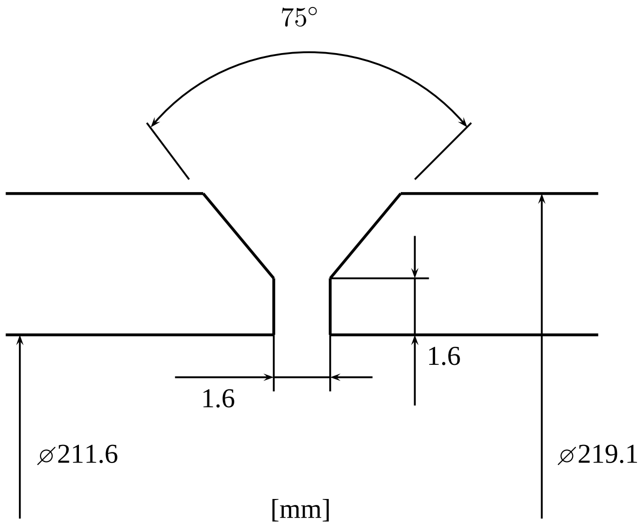

Figure 4.0.2: *Weld groove for both flange models.*

The simulations are all axisymmetric in ANSYS and hence no 3D simulations, since they are both time and CPU expensive. But the author is aware of the assumptions made, as discussed previously, and these simulations should only be used as a comparison, to investigate why one geometry behaves the way it does and how the way the parts are fixed will effect the distortion.

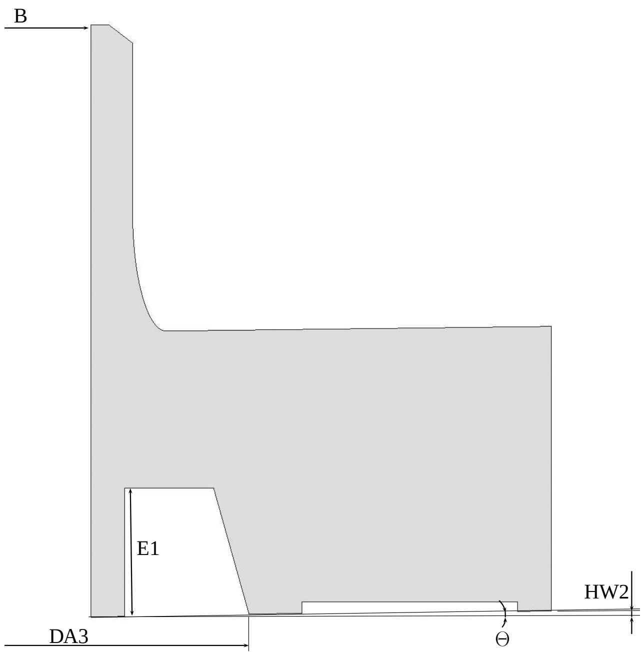

Figure 4.0.3: *Dimensions of interest.*

The dimensions of interest on the flange is shown in Figure 4.0.3. The displacements and rotations of these dimensions have been measured before and after welding on two sets of flanges for both models [14]. B and DA3 are diameters, E1 and HW2 are distances and Θ is an angle.

4.1 Analytical predictions

This section provides a quick analytical method of predicting the difference between the two designs, using elasticity theory from [15]. This theory assumes a evenly distributed twisting moment along the midline, see Figure 4.1.1 this is meant in this short analytical study to simulate the contraction that appears at the weld and gives rise to eversion of the flange. The theory, similarly to beam theory, assumes that the cross section is rigid and will not deform. The relation between the applied twisting moment and the cross sectional rotation can be seen in Equation 4.1.1.

$$M = \frac{E \cdot \Theta \cdot H}{r_0^2} \tag{4.1.1}$$

$$\begin{aligned} &where \\ &\quad M = Evenly\ distributed\ moment\ per\ unit\ length. \\ &\quad E = Young's\ modulus \\ &\quad \Theta = Cross\ sectional\ rotation \\ &\quad H = Cross\ sectional\ stiffness \\ &\quad r_0 = Radius\ to\ the\ cross\ section\ centre\ of\ gravity \end{aligned}$$

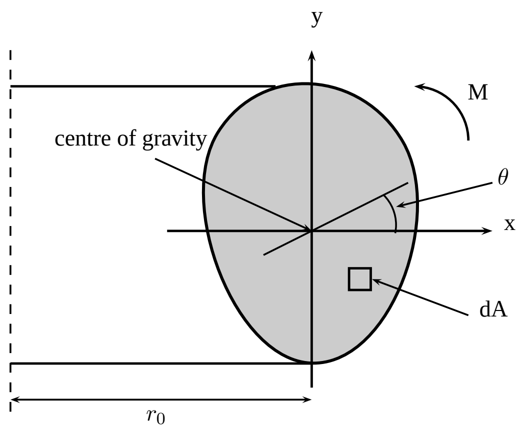

Figure 4.1.1: *Explanation of Equation 4.1.1.*

When the dimensions inside the cross section is small compared to the radius, r_0, H is approximated according to Equation 4.1.2. Using the values for each of the cross sections in Table 4.1.1, the fact that they are made from the same material and assume that both designs will be subjected to the same moment we can combine the Equations for each design and acquire the relation in Equation 4.1.3.

$$H = J_{xx} = \int_A y^2 dA \tag{4.1.2}$$

$$\begin{aligned} &where \\ &\quad J_{xx} = second\ moment\ of\ area \\ &\quad y = the\ perpendicular\ distance\ from\ the\ x\ axis\ to\ the\ area\ dA \end{aligned}$$

$$M_{CRYO} = M_{CL150} \Rightarrow \Theta_{CL150} = 1.618\Theta_{CRYO} \tag{4.1.3}$$

Table 4.1.1: Design properties.

Design	Center of mass(x)	$J_{xx}(\mathrm{m}^4)$
CL150	0.12278	1.09038×10^{-7}
CRYO	0.12566	1.68265×10^{-7}

This implies that when applying the same moment to these two designs, the angle on the CL150 is going to be 1.62 times bigger than it will on the CRYO design.

4.2 Material properties

The material for the pipe and flange is the same, austenitic stainless steel 316L, the material properties for this can be found in Figures 4.2.1 and 4.2.2. The material data for this is collected from [8], with the exception of the tangent modulus which was estimated using [7] and [16]. This type of steel does not experience any solid state phase changes. The filler material used is called Thermanit GE-316L Si, which is assumed to have the same properties as the base material with the yield limit and thermal expansion coefficient as the exception, see Figure 4.2.2a and 4.2.2b. The yield limit for this material is only provided at room temperature and therefore had to be scaled for the other temperatures in respect to the base materials yield limit. The thermal expansion is set to zero at T_{pre} for the filler material, since this is assumed to be added without any stress or strains and should only contract in the weld. As for the base material the thermal expansion is set to zero at the liquidus temperature in order to reduce the thermal load due to convergence issues and the expansion should not have any effect since the material is a liquid at these temperatures with little or no stiffness. The solidus and liquidus temperature are 1420° and 1460°, respectively, and the latent heat of fusion L = 300 kJ/kg [8]. Where the latent heat of fusion is again "spread" out using the effective specific heat, c_{eff} as in previous model. And a high value of the convection is used to simulate the stirror effect in the molten pool for temperatures above the melting point. It can be seen in the figures for the thermal material properties they are assumed to remain constant for temperatures above the liquidus temperature and since the thermal expansion is zero at T_{pre} and the liquidus temperature for the filler and base material respectively, the mechanical effect above these temperatures for each material is excluded.

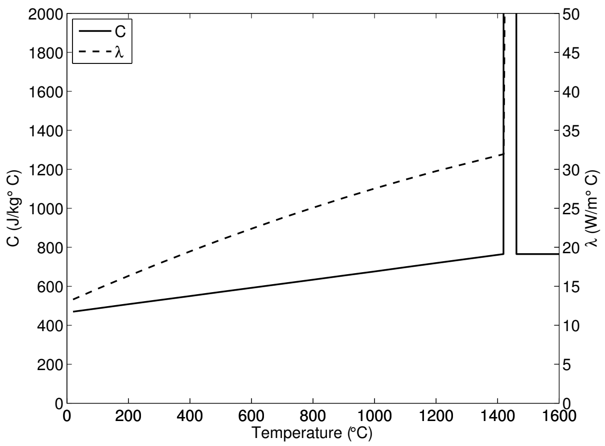

Figure 4.2.1: *Thermal properties of both filler and base material in flange model.*

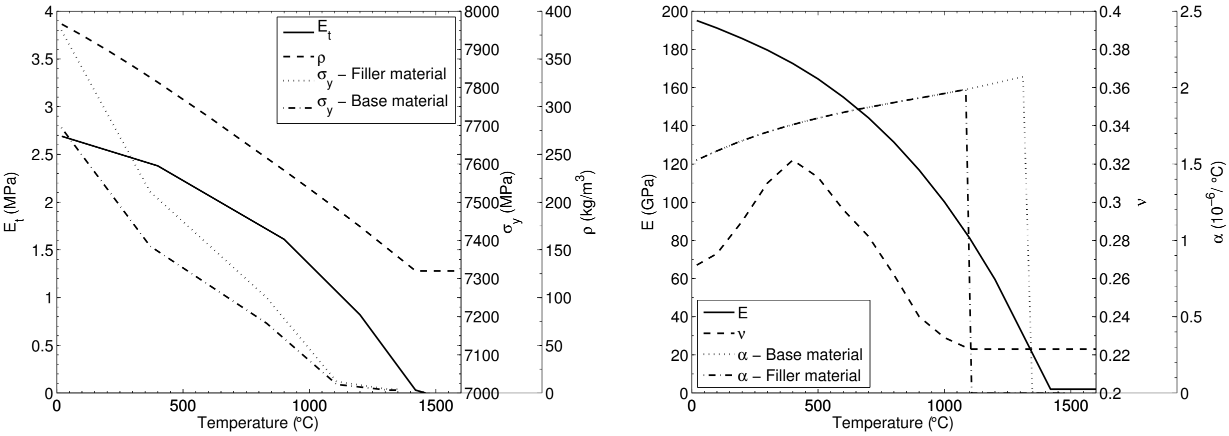

(a) *Tangent modulus, density and yield limit.* (b) *Young's modulus, poisson's ratio and thermal expansion.*

Figure 4.2.2: *Mechanical properties of both filler and base material in flange model.*

4.3 Finite element model

As stated above, both geometries are modeled axisymmetric, the mesh close to the weld is shown in Figure 4.3.1, where the outlines of the three weld passes have been highlighted. This mesh is used for both models, since the geometry in this area is identical. The mesh for the base, were the differences starts, of CL150 and CRYO CL150 is shown in Figure 4.3.2a and 4.3.2b, respectively. The CL150 mesh consists of 5287 elements and 6065 nodes, and the CRYO CL150 consists of 6248 elements and 5464 nodes. The reason for more elements than nodes is that surface elements are used on the edge around the flange which share the nodes of the underlying elements. In Figure 4.3.3 the mesh of both the pipe and flange CL150 is shown. It is not the complete pipe but more than half of it and it displays the consistency in mesh density along the pipe. In both models ANSYS element types Plane55 and Plane182 are used for the thermal and structural analysis respectively, with the same mesh density in both analyses. As in the Andersson model, the elements use four integration points by default, but in the mechanical analysis the option for reduced integration with hourglass control is used in order to prevent volumetric locking.

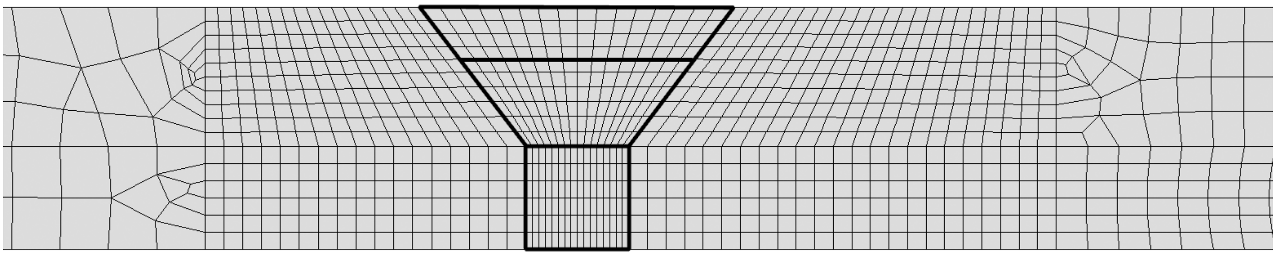

Figure 4.3.1: *Finite element mesh used in the area around the weld groove.*

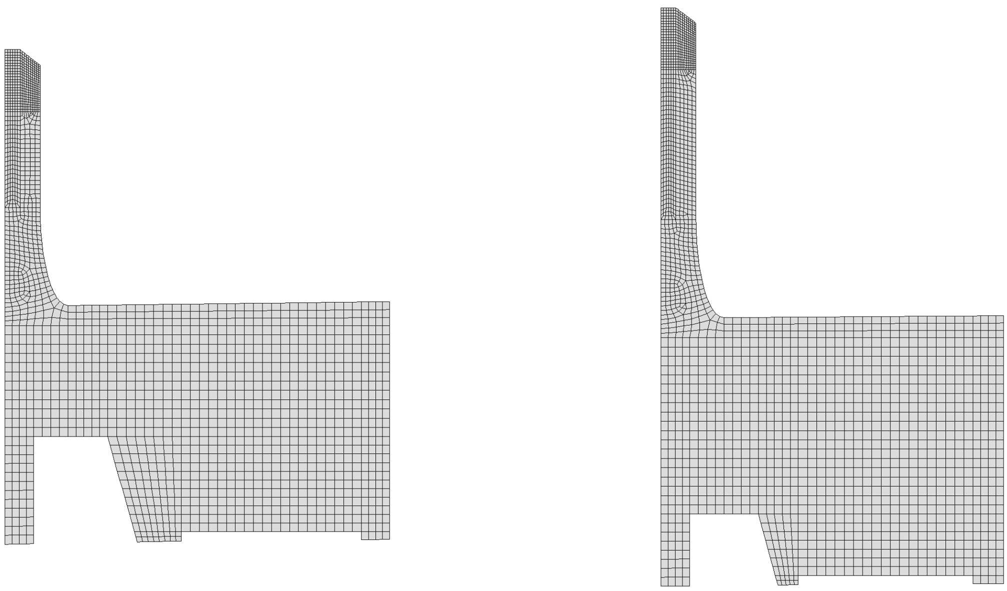

(a) *CL150.*

(b) *CRYO CL150.*

Figure 4.3.2: *Finite element meshes for both flange geometries*

Figure 4.3.3: *Flange and pipe mesh.*

4.4 Thermal analysis

The welding parameters for each weld pass is presented in Table 4.4.1 obtained from [14]. The same procedure is applied as in the Andersson model, using EKILL on weld pass elements not yet deposited, and bringing them back into the model with EALIVE when the weld pass is being deposited. The biggest difference is that this is three separate weld passes, where as in the Andersson model there was three different electrode passing by closely together. This means that there is a pause between the weld passes in the flange analysis, where the minimum time is set by the maximum interpass temperature. In this case this temperature is 150° [13], however the material cools faster below this limit than it takes for the weld to complete one full pass around the whole circumference so the time between two passes are set equal to the time it takes to complete one full pass.

The heat generation applied to each pass is calculated in a similar way as in the Andersson model. Starting with the total heat input using Equation 4.4.1. Where the electrode efficiency is assume to be 0.45.

$$Q_{tot} = \frac{U \cdot I \cdot \eta \cdot l}{v} \tag{4.4.1}$$

The heat content of the filler material is subtracted from the total, since it is added to the model at a temperature of 1200°C, using eq 4.4.2 to work out the amount of energy stored.

$$u_{filler} = T_{pre} \cdot V_{filler} \cdot c_p(T_{pre}) \cdot \rho \tag{4.4.2}$$

Apart from being reduced by the heat content in the filler material Q_{tot} is also divided in Equation 4.4.3 by the weld pass volume it is assumed to be melting, in this case the corresponding filler material volume. This volume is assumed through the weld speed and reasonable weld pool and HAZ sizes since there are no experimental data to compare against. The size is estimated by varying a fraction of the circumference in the same way as [7]. Where a reasonable molten zone is stated to be when at least the melting temperature is reached in all the finite elements that are included in the particular weld pass and the distance to the HAZ from the fusion boundary is stated to be a few mm. The most suitable fraction of the circumference used was 1/11, which with the welding speed specified produces a weld pool length of approximately 10mm.

$$q = \frac{Q_{tot} - u_{filler}}{V_{filler}} \tag{4.4.3}$$

The thermal boundary conditions include both conductivity and radiation for all free surfaces. The convection is assumed to be 13.5 w/m^2C. The radiation emissivity is assumed to be 0.9 and the Stefan Boltzmann constant is set to $5.669 \cdot 10^{-8}$. The thermal boundary conditions follow the ”reactivation” of the elements in the weld, so that cooling also occurs correctly between weld passes. This is achieved by implementing surface elements around the whole model and weld passes and using EKILL/EALIVE to ”activate” and ”deactivate” the boundary conditions at the weld. The element stiffness multiplier, ESTIF, is set in the thermal analysis to 1e-6.

Table 4.4.1: Welding parameters [14].

Weld pass	I ampere	U volt	v mm/min	Heat input kJ/mm
1	95	15	125	0.684
2	110	15	125	0.792
3	110	16	125	0.845

4.5 Mechanical analysis

The thermal history from the thermal analysis is used as the only applied in the mechanical analysis. Finite elements belonging to weld pass two and three are inactive from the beginning. Inactive elements are brought alive 0.05 seconds later in the mechanical analysis in order to achieve convergence over these periods of abrupt changes in the model. The element stiffness multiplier ESTIF is set to 1e-3. The filler material is assigned a reference temperature of T_{pre} to simulate deposition at melted state when activated, and the full Newton-Raphson method with adaptive descent is used.

4.6 Results

The results from the analysis described in previous sections are presented here. The deformed mesh directly after each weld pass is deposited in the CL150 analysis, where the flange is fixed is shown in Figure 4.6.1. Notice that the elements in weld pass three are the most deformed ones, since they are the ones that experience the most deformation when unactivated and having very low stiffness. There are two geometries, CL150 and CRYO CL150, and two different ways of restraining the flange and pipe. The first approach is called pipe fixed in the result tables which means that the flange and pipe is tack welded together to fix them together and the far end of the pipe is fixed. The second approach where the flange bottom is fixed is called flange fixed in the result table. Table 4.6.1 show results for CL150 and Table 4.6.2 for CRYO CL150. Both tables displays the results in millimeters outside the tolerance for each dimension, which is shown in the second column.

The ratio $\Theta_{CL150}/\Theta_{CRYO}$ calculated in the analytical section is included in Table 4.6.3, together with the similar ratio calculated in ANSYS and from the measured values using the inner and outer radius of the bottom of the flange. The assumption in the analytical predictions, that the cross section is rigid, is shown to be true in the ANSYS models, except for the thin neck at the top of the flange.

Table 4.6.1: Flange displacements and rotations - CL150 [mm]

	Allowed deformation	Deformations outside tolerance		
Dimension	(tolerance)	Measured	Pipe fixed	Flange fixed
⌀DA3	0.1	0.121	0.065	0.000
HW2	0.04	0.303	0.242	0.000
⌀B	-0.1	0.000	1.849	2.287
E1	0.15	0.000	0.000	0.000

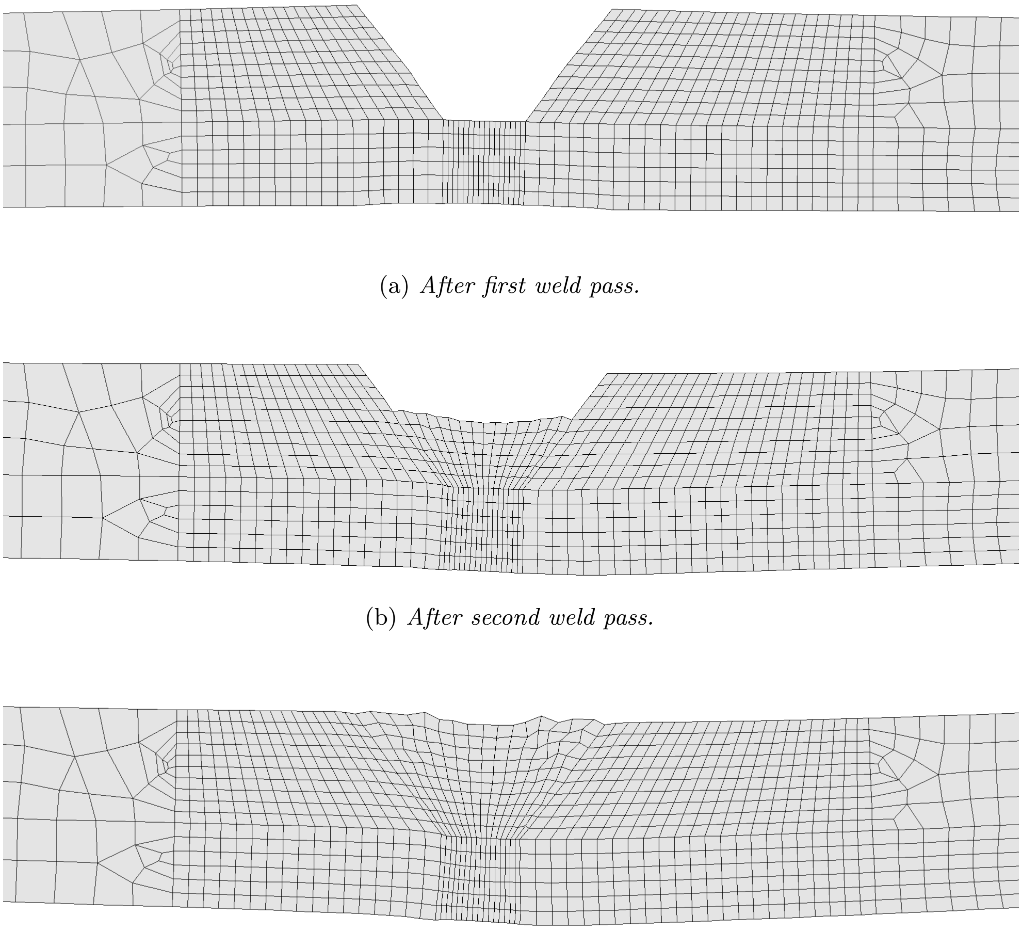

(a) *After first weld pass.*

(b) *After second weld pass.*

(c) *After third weld pass.*

Figure 4.6.1: *Deformed mesh after each of the three weld passes for CL150 with a fixed flange.*

Table 4.6.2: Flange displacements and rotations - CRYO CL150 [mm]

Dimension	Allowed deformation (tolerance)	Deformations outside tolerance Measured	Pipe fixed	Flange fixed
⌀DA3	0.1	0.095	0.006	0.000
HW2	0.02	0.055	0.121	0.000
⌀B	-0.1	0.495	2.039	2.256
E1	0.15	0.000	0.000	0.000

Table 4.6.3: Flange Θ results

Ratio	Measured	Analytical	FEM/ANSYS Pipe fixed	Flange fixed
$\Theta_{CL150}/\Theta_{CRYO}$	2.174	1.618	1.776	1.509

5 Discussion

This chapter discusses the models in general and each model separately as well as ANSYS ability to conduct welding simulations and notes for future work.

5.1 Andersson model

The results from the Andersson model shows good agreement with those measured by Andersson. The temperatures at points A and B differs from the measured ones somewhat, but the difference is small in the context and is assumed not to affect the results. The stress results on the upper side of the plate shows good agreement for the longitudinal stress in the weld direction, z. Whereas the stress in the transverse x-direction deviates both from the measured and calculated stresses from Andersson close to the weld. Tensile stresses appear where compressed are expected from the measurements. Since this is the most complex region to model and not all of the parts of the Andersson model was included in this simulation due to convergence issues it is no surprise that the stresses deviate in this area. Andersson explains his deviations from the experimentally measured values as a result of the assumption of generalized plane strain and the stresses induced by the hold down clamps. These reason are of course true in the present analysis as well. The lower side shows good agreement over the whole distance range, even though the model has some major differences than the original by Andersson. The lower side is of course easier to predict since the heat is not that intense in this region. The fact that most of the stress results seems offset to Anderssons stress results by the same amount could be because that theses stresses and the measured ones where extracted from a small diagram not created digitally. Another source for differences in results could be boundary conditions use, since it could not be found in his article how he constrained the model, it was assumed in this thesis that the lower corner of the cross section at the far end of the plate was fixed.

As mentioned previously Lindgren also repeated this simulation in [12], and compared to the results in the present study the results agree well. Lindgren examined different models, trying to explain and reduce the difference between measured and calculated residual stresses but did not succeed in doing so. Those results(not presented in this thesis) show a slightly higher residual stress in the longitudinal direction on the upper surface for x >50mm than in the present study and the transverse residual stresses shows similar results to Andersson and those calculated in this study. The different models used by Lindgren produces the same residual stress, they provide only a difference close to the weld in the transverse stresses. Lindgren states that the reason for the difference between measured and calculated could be because of the simplification that it is made two-dimensional.

Even though the results do look promising there are some aspects that are reason for concern. The temperatures for example shows good agreement with experiments, see Figure 3.5.2, but the temperatures close to the weld are very high. The temperature in the fusion zone after the third electrode passed shows temperatures over $2.5 \cdot T_{liquidus}$, which is extreme. These results where not included in the results section since there where no data to compare with, and Andersson does not state any temperature in the fusion zone, which means he might have got the same. But, measurements made, though not in this case, show that the temperature in the weld pool rises to temperatures $300 - 500°C$ above the melting point [17]. Another odd observation on Andersson's model is the use of a very small number for the emissivity, 0.004939, where values between 0.5 to 0.9 are not uncommon. Smaller values do exist, but lower than 0.02 is very unusual. The best explanation is that Andersson could have used the emissivity as one tuning variable to acquire the correct temperature field. Simulations made in the present analysis showed that with a significantly higher emissivity results in larger temperature differences compared to measured ones.

5.2 Flange models

From the two flange models we can see that the results do reflect the reality experienced at Vector Technology Group AS. The CRYO CL150 model is more resistant against eversion, when the models are simulated as tack welded to the pipe, even though it has a smaller tolerance value. But the tolerance limit is not reached for more than one dimension for both designs. Both designs however show significant improvement when the other boundary condition is used, where the flange is fixed, and passes the tolerance limit for all but one dimension, discussed later. This shows that the CRYO CL150 model is stiffer and will deform less after welding, but it also shows that the way the pipe and flange is held in place during is most likely equally important in this case.

Moving on to the dimension that none of the models could reach within the drawing tolerance, the $\varnothing$B. The reason for that the measured one falls within the tolerance limit and not the finite element models, from the looks of the measurement protocols provided, is because option 3 is used to hold the pipe and flange together. Since from these protocols this measurement, which is the inner diameter of the flange right at the weld, is getting larger after the weld has taken place. This would not be possible if there was not something on the inside applying a pressure in the vicinity of the weld. As stated earlier this was not implemented in the present thesis, since it would have involved complex contact elements with heat transfer, which is outside the scope of this thesis.

The cross sectional rotation, θ, estimated from analytical calculation of a non-deforming cross section, measured and calculated using ANSYS also shows that the CRYO model is stiffer. The analytical and calculated results for the rotation in ANSYS shows good agreement, but the measured one stands out. This could, again, be a result of the fact that a different method was used to hold the pipe and flange during welding was used, but since this is a ratio between the two designs it should not matter if the procedure was the same. The reason for the discrepancy between the analytical and ANSYS values are most likely a result of the analytical theory. Which assumes that the cross section is rigid and will not deform, but that is allowed in the finite element model in ANSYS. This shows once again that the CRYO CL150 model is in fact stiffer, but that this extra stiffness is not critical when fixing pipe and flange in a proper way.

5.3 ANSYS

The enthalpy method discussed in a previous chapter was given a chance and was implemented in the Andersson model, since it is preferable as it reduces the nonlinearity when the latent heats are released or absorbed in the model. ANSYS does have the capabilities for this but convergence could not be achieved. The time to solve the thermal analysis would probably have been reduced and the whole model would become more time-efficient and stable to solve.
The fact that the thermal dilatation curve could not be implemented in the Andersson model, even though only one was sought to be implemented, is somewhat worrying. This curve is nonlinear so this is of course one reason for not obtaining a solution. But even when efforts where made to smooth out these nonlinearities it could not provide a solution. This does makes ANSYS difficult to use when handling welding of materials which undergoes solid-solid phase changes, e.g. ferritic steels.
The overall experience of ANSYS is that the welding simulations are very sensitive, especially the mechanical analysis at times when elements are activated. Which is understandable since this is big changes in the model, and often together with high temperatures. And it is hard to say if this is always the case when solving welding simulations or if it has to do with ANSYS since the author

have no experience in welding simulation in any other software. But the fact the only a few papers have been published on the subject with ANSYS as the software, might be another indication of its suitability for this purpose.

5.4 Future work

Modeling the heat source was one of the biggest challenges during development of these models. Partly because no experimental results was available in one case but also the fact that it is a three-dimensional heat flow. Reducing this to only two dimensions is very difficult, and the acquired thermal results are suspicious in some cases, most likely as a result of this. Modeling in three-dimensions would remove this problem and uncertainties associated with it, however there is still the issue of time and computational resources. The recommendation would be to improve the heat source modeling as much as possible when conducting welding simulations. As soon as the three-dimensional modeling becomes viable this should be used. And appropriate would be to use a more complex shape and intensity of the heat source than the constant area heat source used in this thesis. The Gaussian, double ellipsoid is one example of a more accurate model available for this purpose [18]. Another way of increasing the accuracy of the thermal analysis is to do that analysis three-dimensionally and select a cross section, extract the temperature history from that cross section and apply it to the two-dimensional mechanical analysis. This will increase the computational time and user interaction between the thermal and mechanical analysis, but since the thermal analysis uses one degree of freedom per node it is manageable compared to the mechanical one. Using this approach would allow a much better temperature history without the issue making a three-dimensional problem two-dimensional.

For future simulation of flange models in ANSYS it is recommended to revise the welding parameters used in the weld process and make a detailed comparison of the molten zone and HAZ between an experiment, ANSYS and a second finite element package. To ensure that the ANSYS model accurately describes what is happening near the weld and also to set a more narrow welding specification, since the current one allows the heat input to be increased by 75% and still be inside the limit. This is most likely because the specification should be valid for more than one set of flange and pipes. It is also recommended that along with more specified welding parameters to also specify how the flange and pipe parts are fixed, since the results shows that it has great influence on the deformations after welding. And of course implement this in ANSYS as well.

6 Conclusions

One two-dimensional numerical model has been developed to examine the welding simulation capability in ANSYS. The simulation of Andersson [5] was revisited and results was compared to Anderssons simulation and experiments. The entire model could not be implemented and the discrepancies in the results are most likely caused by this. This model and the results show that ANSYS is able to simulate welding, though with some limitations and difficulties. The ability to use EKILL and EALIVE commands provides a convenient way of adding filler material. But modeling solid to solid phase change could not be implemented and for simulations requiring this ANSYS is not recommended.

Two axisymmetric flange models was developed to examine the welding deformations for the designs, as well as determine the effects of how the flange and pipe are restrained during welding. Two different ways of restraint was examined, while undergoing the same welding procedure. The simulations from ANSYS together with a simple analytical predictions shows that the CRYO design is the preferred one considering welding deformations. This is also supported by the available measurements before and after welding of both flanges. However, it was also found that it is equally important how the flange and pipe are fixed during welding, when applying the proper boundary condition the difference between the designs becomes very small. It is therefore necessary to establish specific procedures and demands on the welding process in order to reduce the welding deformations.

References

[1] L.-E. Lindgren. "Finite Element Modeling and Simulation of Welding Part I: Increased Complexity". *Journal of Thermal Stresses* **24** (2001), pp. 141–192.

[2] K. Weman. *Welding processes handbook.* Woodhead Publishing Ltd, 2003.

[3] L.-E. Lindgren. "Finite Element Modeling and Simulation of Welding Part 2: Improved Material Modeling". *Journal of Thermal Stresses* **24** (2001), pp. 195–231.

[4] R. Lewis, K. Morgan, H. R. Thomas, and K. Seetharamu. *The Finite Element Method in Heat Transfer Analysis.* John Wiley & Sons Ltd, 1996.

[5] B. A. B. Andersson. "Thermal stresses in a submerged-arc welded joint considering phase transformations". *ASME Journal of Engineering Materials and Technology* **100** (1978), pp. 356–362.

[6] A. Capriccioli and P. Frosi. "Multipurpose ANSYS FE procedure for welding process simulation". *Fusion Engineering and Design* **84** (2009), pp. 546–553.

[7] B. Brickstad and B. L. Josefson. "A parametric study of residual stresses in multi-pass butt-welded stainless steel pipes". *International Journal Of Pressure Vessels and Piping* **75** (1998), pp. 11–25.

[8] P. Dong. "Residual Stress Analyses of a Multi-pass Girth Weld: 3-D Special Shell Versus Axisymmetric Models". *Journal of Pressure Vessel Technology* **123** (2001), pp. 207–213.

[9] L.-E. Lindgren, H. Runnemalm, and M. O. Näsström. "A New Finite Element Model for Welding Heat Sources". *Metallurgical and Materials Transactions B* **15** (1984), pp. 299–305.

[10] T. Haraldsson and S. Larzenius. "Calculation of Welding Residual Stresses in a Cladded Thick-Walled Plate". Master's Thesis no 2006:17. Applied Mechanics, Division of Material and Computational Mechanics, Chalmers University of Technology, 2006.

[11] *ANSYS Mechanical.* Version 14.0. ANSYS, Inc., Canonsburg, PA, USA.

[12] L.-E. Lindgren. "Finite Element Modeling and Simulation of Welding Part 3: Efficiency and Integration". *Journal of Thermal Stresses* **24** (2001), pp. 305–334.

[13] P. Lindström. Private Communication. Per Lindstrom Engineering, 2012.

[14] Private Communication. Vector Technology Group AS, 2012.

[15] B. Sundström, ed. *Handbok och formelsamling i hållfasthetslära.* Institutionen för hållfasthetslära, KTH, 1998.

[16] O. Muránsky, M. Smith, P. Bendeich, T. Holden, V. Luzin, R. Martins, and L. Edwards. "Comprehensive numerical analysis of three-pass bead-in-slot weld and its critical validation using neutron and synchrotron diffraction residual stress measurements". *International Journal of Solids and Structures* **49** (2012), pp. 1045–1062.

[17] J. A. Goldak and M. Aklaghi. *Computational Welding Mechanics.* Springer Science+Business Media, Inc, 2005.

[18] J. A. Goldak, A. Chakravarti, and M. Bibby. "A New Finite Element Model for Welding Heat Sources". *Metallurgical and Materials Transactions B* **15** (1984), pp. 299–305.

[19] R. I. Karlsson and B. L. Josefson. "Three-Dimensional Finite Element Analysis of Temperatures and Stresses in a Single-Pass Butt-Welded Pipe". *Journal of Pressure Vessel Technology* **112** (1990), pp. 76–84.

[20] Z. Barsoum. "Residual stress analysis and fatigue of multi-pass welded tabular structures". *Engineering Failure Analysis* **15** (2008), pp. 863–874.

[21] Z. Barsoum and I. Barsoum. "Residual stress effects on fatigue life of welded structures using LEFM". *Engineering Failure Analysis* **16** (2009), pp. 449–467.

[22] M. Jonsson and B. L. Josefson. "Experimentally determined transient and residual stresses in a butt-welded pipe". *Journal of Strain Analysis* **23** (1988), pp. 25–31.